

INTERNATIONAL SOCIETY FOR SOIL MECHANICS AND GEOTECHNICAL ENGINEERING



This paper was downloaded from the Online Library of the International Society for Soil Mechanics and Geotechnical Engineering (ISSMGE). The library is available here:

<https://www.issmge.org/publications/online-library>

This is an open-access database that archives thousands of papers published under the Auspices of the ISSMGE and maintained by the Innovation and Development Committee of ISSMGE.

The paper was published in the proceedings of the 11th International Conference on Scour and Erosion and was edited by Thor Ugelvig Petersen and Shinji Sassa. The conference was held in Copenhagen, Denmark from September 17th to September 21st 2023.

3D CFD LES process-based scour simulations with morphological acceleration

Lynnyrd de Wit,¹ Desiree Plenker,² and Yorick Broekema³

¹Deltares, Department of Ecology and Sediment Dynamics, Boussinesqweg 1, 2629 HV Delft, the Netherlands; e-mail: Lynnyrd.deWit@deltares.nl Corresponding author.

²Deltares, Department of Hydrodynamics and Offshore Technology, Boussinesqweg 1, 2629 HV Delft, the Netherlands; e-mail: Desiree.Plenker@deltares.nl

³Deltares, Department of Hydrodynamics and Offshore Technology, Boussinesqweg 1, 2629 HV Delft, the Netherlands; e-mail: Yorick.Broekema@deltares.nl

ABSTRACT

Process-based 3D CFD (Computational Fluid Dynamics) scour simulations with open-source software TUDflow3D are presented for a square and round monopile and a jacket foundation. The Large Eddy Simulation (LES) approach is used to capture the unsteady turbulent flow and vortices associated with flow around obstacles. Morphological acceleration is applied to speed up the bed-evolution and keep computational times feasible. With an acceleration factor 100 accurate results are obtained, but 100 times faster. Both spatial and time development of the simulated scour compares well with the measured scour in lab experiments. Our paper shows that process-based 3D CFD scour simulations with morphological acceleration can provide accurate results in just a couple of days computational time on an 8-core computer. This makes process-based CFD scour simulations feasible for engineering projects.

INTRODUCTION

With increasing computational power as well as advanced numerical software, numerical process-based simulation of scour becomes feasible. Detailed unsteady Computational Fluid Dynamics (CFD) simulations of flow past obstacles are done for decades already with satisfactory results and revealing many details of the flow, see for example but far from complete Rodi (1998), Krajnovic (2002,2011), Yeon (2014). More recently also process-based morphodynamic simulations of scour round an obstacle are carried out, see for example and again not complete Roulund et al. (2005), Kim & Nabi (2014), Baykal et al. (2017). Numerical process-based simulation of scour can supplement experimental investigations to limit the amount of experiments or to use for circumstances which are difficult to investigate in an experiment and can provide an abundance of 3D data without interfering with the flow. This paper presents process-based 3D CFD scour simulations for square and round monopiles and a jacket foundation. The Large Eddy Simulation (LES) approach is used to model the turbulent flow. An advantage of the LES approach over RANS (Reynolds averaged Navier Stokes) is that it resolves the large coherent turbulent structures instead of solely mimicking the effect of those coherent structures by a large eddy viscosity.

Especially for flow past an obstacle resolving the large coherent structures is an advantage to capture the unsteady turbulent flow and vortices associated with flow around obstacles. To keep computational times feasible, morphological acceleration is applied to speed up the bed-evolution without changing the flow parameters and in this manner decouple the morphological and flow timescales. With an acceleration factor of 100 accurate results are still obtained, but 100 times faster. Aim is to show that accurate CFD scour results are achievable not only on a super-computer with thousands of cores and months of computational time, but instead on a workstation within a couple of days.

CFD MODEL TUDFLOW3D

General

CFD model TUDflow3D has been developed originally for dredge plume investigations (De Wit, 2015). Based on this background, the model can deal with multi-fraction suspended sediment including variable density influences and highly turbulent flow. It has been validated for a wide range of applications and flow conditions, such as buoyant jet in crossflow, turbulent channel flow with and without suspended sediment, flow past obstacles, density currents and dredge plumes (De Wit, 2015). TUDflow3D is an open-source code available on <https://github.com/openearth/tudflow3d>.

Flow solver

In TUDflow3D the full 3D Navier-Stokes equations are solved including variable density:

$$\frac{\partial \rho}{\partial t} + \nabla \cdot (\rho \mathbf{u}) = 0,$$

$$\frac{\partial \rho \mathbf{u}}{\partial t} + \nabla \cdot (\rho \mathbf{u} \otimes \mathbf{u}) = -\nabla P + \nabla \cdot \boldsymbol{\tau} + (\rho - \rho_a) \mathbf{g},$$

where ρ, ρ_a is respectively the mixture density and density of ambient water, \mathbf{u} is the 3D velocity vector, t is time, P is the dynamic pressure, $\boldsymbol{\tau}$ is the viscous shear stress tensor and \mathbf{g} is the gravitational acceleration vector.

The simulations are carried out using a second order accurate finite volume method on a structured grid using a rigid lid. The use of structured grids allows the use of a rapid solver. The code runs parallel (domain decomposition via MPI) on multicore computers for maximum speed. The influence of suspended sediment on mixture density is captured by the mixture model approach (Manninen et al., 1996). The pressure correction technique is used to enforce incompressibility following from the mass balance. Time integration of the advective, viscous, old pressure and body force terms during the predictor step is carried out by a third order Adams-Bashforth scheme. Momentum advection is simulated using a stable artificial viscosity scheme (De Wit and Van Rhee, 2014). The WALE LES sub-grid scale model (Nicoud and Ducros, 1999) with $C_s=0.325$ is used to capture the influence of turbulence. For the first fluid cell above the bed a minimum

viscosity is applied to be able to provide the required bed shear stress $\tau_{sgs} \geq u^* \cdot \left. \frac{\partial U}{\partial z} \right|_{z=z_{bed}}$. Since the LES approach is used, special care is taken for the conditions at the inlet by assigning realistic turbulent fluctuations (Jarrin et al., 2006). For more details see De Wit (2015).

Sediment pickup, bedload and avalanche functions

TUDflow3D simulates sediment suspension load and bedload transport. Suspension load is simulated by a 3D sediment transport equation. At the bed suspended sediment can erode and deposit. In the cases of this study a single fraction with sediment size equal to the d_{50} is used, but it is possible to use more fractions. A sediment pickup function based on Van Rijn (1984) is used for the determining the erosion flux at the bed. The deposition flux at the bed consists of the suspended sediment concentration in the lowest computational cell multiplied by the settling velocity. Hindered settling correction is included, although this is only relevant for very high concentrations which do not occur in this study.

Bedload is simulated by a bedload formula based on Van Rijn (2007) and the bed-update resulting from the spatial gradients in the bedload transport is added to the bed-update from the suspension load. For the bedload a bed-slope correction is applied for the longitudinal slopes according to Bagnold (1966) with a default setting of $\alpha_{bs}=1$.

The bed shear-stress of flow and suspension pickup is used in an instantaneous manner and the bed shear-stress of the bedload is smoothed in time by a relaxation factor 0.01 applied on the near bed velocity. The sediment bed shear-stress is determined with the flow velocity of the first computational cell from the bed which is between $0.5-1.5 \cdot \Delta z$ from the bed. The velocity component parallel to the local bed-slope is used and the pickup acts perpendicular to it.

An avalanche routine is included to prevent the development of unrealistically steep bed slopes. When the bed slope of any two neighboring cells gets steeper as the user defined avalanche slope then sediment is moved from the high to the low bed as a form of instantaneous bedload to arrive back at the avalanche slope.

Immersed boundary method for obstacles and bed update with morphological speedup

Obstacles and the sediment bed within the grid are treated with an immersed boundary method (IBM) which forces the flow velocity of cells inside the bed or obstacle to zero. Obstacles use a first order IBM where a computational cell is either completely fluid or completely obstacle with zero velocity. At the sediment bed a second-order accurate IBM is used in which the exact vertical position of the bed-level (not rounded off to the nearest complete filled cell) is used to determine the impact on the flow and to determine the bed shear-stresses.

The bed level can vary during the simulation because of erosion and deposition of suspended sediment and spatial gradients in the bedload transport. The response of the flow field on the bed-level changes is determined by taking exactly the linear interpolated bed-level into account. To have a robust, accurate and sediment mass-conserving treatment of the bed composition without a cell flipping from erosion to deposition or vice versa multiple time steps in a row, the bed level can vary seamlessly between $-0.5 \cdot \Delta z$ to $+0.5 \cdot \Delta z$ around the topmost cell of

the bed. When the bed level gets below $-0.5\Delta z$, the topmost computational bed cell is lowered one layer, while the topmost bed cell is raised by one layer if the bed level gets above $+0.5\Delta z$. In the range of 0 to $+0.5\Delta z$ the top bed-cell is completely filled with a flexible buffer bed sediment layer, filled with the right composition and amount of sediment to account for the last 0 to $+0.5\Delta z$. In the range of $-0.5\Delta z$ to 0 the sediment content of the top bed-cell is reduced to half with the remaining part in the flexible buffer bed sediment layer. A schematization of this approach is illustrated in Figure 1. This approach gives the benefit of sediment mass-conservativeness and accommodates a gradual transition from $-0.5\Delta z$ to $+0.5\Delta z$ without a cell repeatedly flipping from erosion to deposition state or vice versa.

Morphological acceleration is applied to speed up the bed-evolution and keep computational times feasible. This is allowable because morphological bed evolution takes place at a time scale which is much slower than the turbulent flow time scale. With an acceleration factor 100 accurate results are obtained for the cases considered in this paper, but 100 times faster.

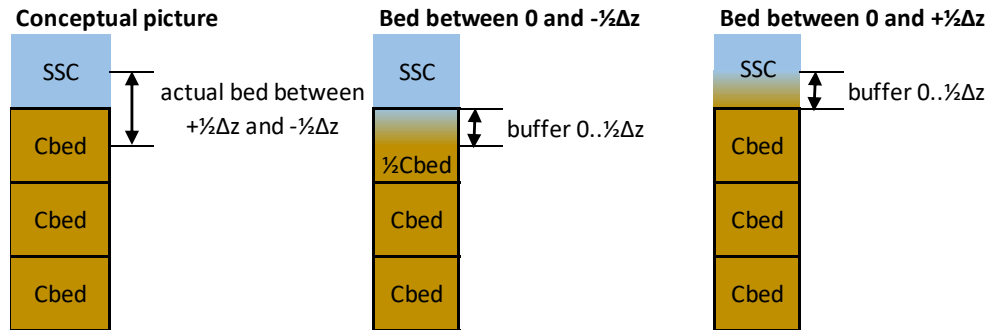


Figure 1. Conceptual picture of the sediment bed composition at the fluid-sediment interface with continuously varying bed levels. The IBM feedback on the flow is calculated with the exact bed-level.

APPLICATION OF TUDFLOW3D FOR SCOUR SIMULATIONS

Three different scenarios of scour behind obstacles with increasing complexity are simulated with TUDflow3D to prove the capability to simulate scour in a process-based manner efficiently. The three cases considered, are scour hole development at monopile foundations (square and round) and a jacket foundation. Validation data of the measured scour in laboratory tests is available to assess the quality of the CFD results. Before starting morphological scour simulations, the ability of TUDflow3D to simulate flow past a round monopile was validated (not shown) with flow experiments from Roulund et al. (2005) and Hinterberger (2004) and several more general test cases of flow past an object are reported in De Wit (2015) and Radermacher et al. (2016).

The pickup and bedload functions in any morphological model give room for calibration, to optimize the model to the specific application. The intention was to derive one set of calibration parameters for all presented cases. The following calibration set is used for all simulations:

- Bed shear-stresses of flow, suspension pickup and bedload are determined with $2.5\tau_{50}$;

- Suspension pickup calibration factor = 1; Bedload calibration factor = 1.
- Avalanche slope 32 degrees (observed end bed slope in the experiment)

This calibration parameter set is very close to the default values and the results were found to be only a little dependent on the exact choice in parameters. This gives confidence in the applied morphological framework in the CFD model.

CASE 1 & 2: MONOPILES

Case description

The first test cases represent scour development due to flow past a square and a round monopile with diameter $D=0.15\text{m}$. The applied flow velocity is 0.3 m/s with a water depth of 0.75 m and a sand bed with $d_{50}=180\text{ }\mu\text{m}$, which gives a Reynolds number of $Re_D=45,000$. The simulation mimics the original physical test setup, which concerns a 5 h scour development.

The applied CFD cell size is $\Delta x, \Delta y = D/40$ near the monopile, gradually increasing in size further away from the monopile. The vertical cell size is uniformly $\Delta z = D/40$. The model domain covers $x = -5D$ to $13D$ and has a width of $21D$. The total number of grid cells is ~ 14 million.

Model results compared with measured scour

The temporal scour development at different locations next to the square monopile is shown in Figure 2. The CFD model is able to simulate the time development of the scour in a very accurate manner. The fast initial scouring in the first half hour is modelled precisely as well as the slower continuation of scouring in the following 4.5 h . The difference in scour development at different locations round the square monopile is also captured nicely in the CFD simulations. While on the leeside of the monopile (angle= 180°) initially sedimentation takes place before the scouring starts, on the monopile front as well as at its sides the scouring starts almost immediately (see Figure 2).

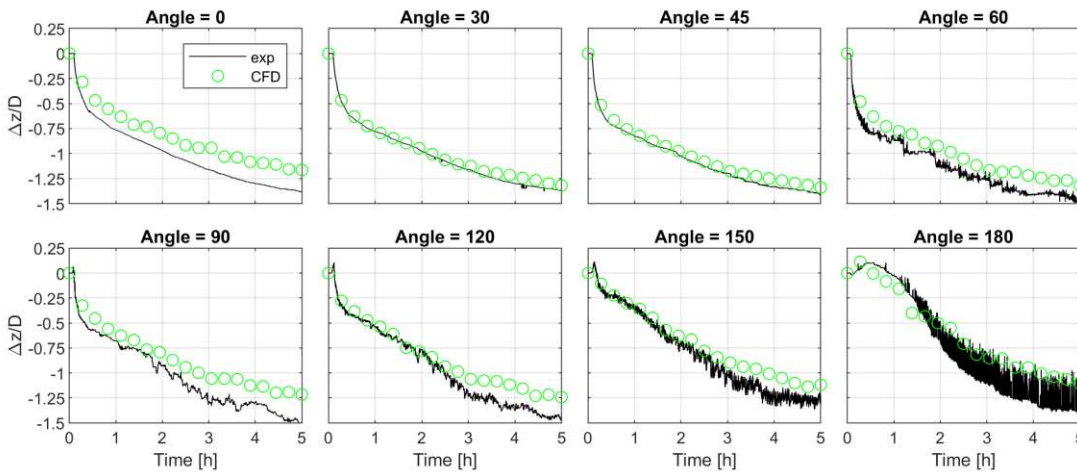


Figure 2. Temporal scour development for different locations directly next to the square monopile; experiment (black line) and CFD (green circles); angle indicates the location: f.i. angle=0 is front, 90 is on the side and 180 is on its leeside.

For the round monopile the CFD model is equally well able to simulate the time development of the scour hole, see Figure 3. The fast initial scour in the first half hour at the sides (angles between 30° and 120°) is captured by the CFD model. However, at the front (angle = 0°) and at the leeside of the round monopile (angle = 150° and 180°) the initial scour development is underpredicted. The slower scouring in the last hours of the experiment is modelled correctly for all angles and the resulting final scour depth after 5 h is also simulated accurately for all angles.

The flow acceleration driven scour at the sideward edges of the monopile is easier to reproduce by the CFD model than the vortices driven scour at the front and back of a monopile. For both, the square and round monopile, the results at the sides are better than the results upstream (angle= 0°) or downstream (angle= 180°), although also in these areas the deviations between CFD and experiment are small.

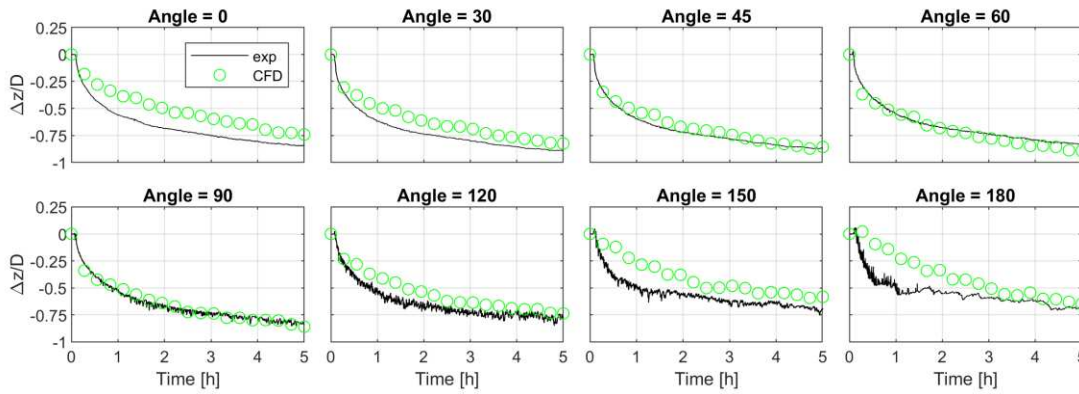


Figure 3. Temporal scour development round monopile, see Fig. 1 for explanation of figure

Sensitivity analysis on grid-size

For the round monopile case a sensitivity analyses on grid resolution is performed by a simulation with higher ($\Delta x, \Delta y, \Delta z = D/70$ near the monopile) and a coarser resolution ($\Delta x, \Delta y, \Delta z = D/25$). The results in case of the coarse grid deviates RMS=10 mm in bed development from the original results with $\Delta x, \Delta y, \Delta z = D/40$. This is equivalent to 8% of the average final scour depth. The RMS difference is determined for 360 locations (1 per degree) adjacent to the monopile for 19 flow files during the 5h scour development. The fine simulation is still running due to cluster issues, but during the first 4h of scour development the deviation is just RMS=8mm. Hence, the results are grid-size independent and the chosen grid size is sufficient for accurate scour simulations.

CASE 3: JACKET

Case description

Last case considers the scour development round an offshore jacket with an outer extent of $D_{\text{jacket}}=1$ m. This is a much more complex shape as the square or round monopile. The jacket considered in this test is shown in Figure 4 (left and middle). It stands on four legs, of which each is founded on two small round foundation piles with a triangular plate on top of the initial bed. The applied flow velocity is 0.47 m/s with a water depth of 0.72 m and a sand bed with $d_{50}=170 \mu\text{m}$, which results in a Reynolds number of $\text{Re}_{D_{\text{jacket}}}=470,000$. The simulation recreates the duration of the experiment with 0.83 h scour development.

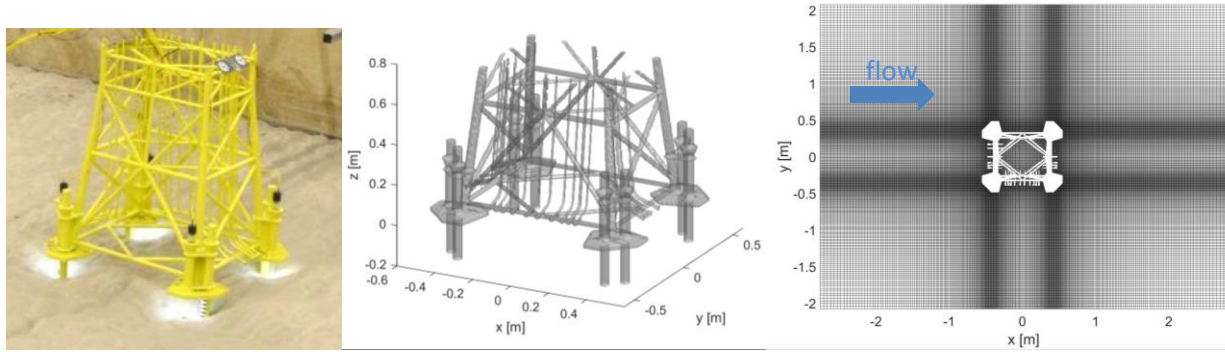


Figure 4. Jacket used in test case 3, picture experiment (left), jacket in CFD model (middle) and horizontal CFD grid (right).

The jacket pipes, auxiliary pipes, four plates and eight small foundation piles are simulated via the immersed boundary method in TUDflow3D on a 22 million cell grid with horizontal grid size $\Delta x, \Delta y = D_{\text{foundation pile}}/8 = D_{\text{jacket}}/200$ near the four jacket foundations, gradually coarsening further away, see Figure 5 (right). The vertical grid size is uniformly $\Delta z = D_{\text{foundation pile}}/8$. The model domain covers $x = -3D_{\text{jacket}}$ to $+3D_{\text{jacket}}$ and has a width of $4D_{\text{jacket}}$.

Model results compared with measured scour

The simulated spatial scour development at the end of the experiment after 0.83h is shown in Figure 5. Below, in between and behind the front jacket legs erosion holes have formed which extent towards the end of the jacket. Behind the leeside jacket legs a deposition zone has developed.

In Figure 6 the simulated scour next to the foundation piles of the jacket is compared with the scour measured in the experiment. Not only the jacket shape is much more complex as previous tests, also the sheltering influence of the plate on top of the bed makes this situation more difficult. At the start of the test the plate prevents scour next to the foundation piles. However, when time passes, edge scour round the plates will develop and the sediment bed below the plates will get exposed to the flow and subject to scour.

This sheltering influence by the plates is also clearly visible in the CFD outcomes in Figure 6. The inner pile downstream remains sheltered during the full experimental duration and

does not show any significant scour. For the outer pile downstream scouring starts after approx. 0.25 h, while for the inner upstream pile scouring starts at 0.1 h. At the outer upstream pile the scouring starts after 0.05 h. Hence, the inner piles stay sheltered longer than the outer piles and the downstream piles stay sheltered longer than the upstream piles. The scour behavior predicted by the CFD model is close to the observed scour development in the experiment. For all four piles the scour rate in time is simulated accurately. For two out of three piles the start of scour is predicted correctly. For the third pile (outer downstream) the predicted scour rate is correct, but it starts 0.25 h too late in the simulation. For the fourth pile, the inner downstream one, the CFD model accurately predicts no scour. Also, the variation in scour over the circle round each pile from the CFD model is close to the experiment. This is indicated in grey for the experiment and with the green vertical lines for the CFD results. All in all, the simulation results for this complex case are very satisfactory.

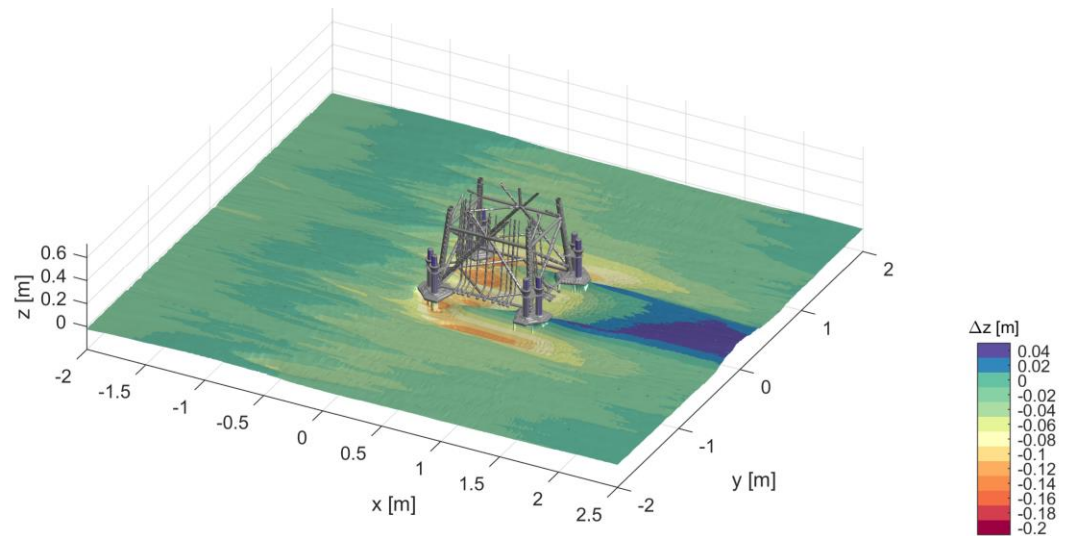


Figure 5. Simulated spatial scour pattern round a jacket after 0.83h scour development.

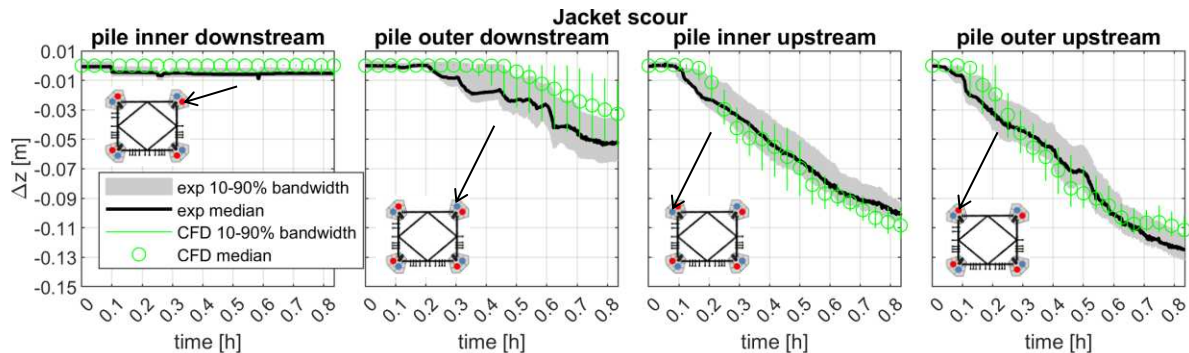


Figure 6. Temporal scour development of 4 different foundation piles of a jacket; experiment (black line) with 10-90% bandwidth (grey) and CFD (green circles) with 10-90% bandwidth (green vertical lines); the 4 locations are indicated with arrows.

MORPHOLOGICAL ACCELERATION

Morphological acceleration was applied to keep the simulation times within limits. Sensitivity of the results on the choice of morphological acceleration factor is investigated by running alternative simulations with a factor 50 and 200 for the round monopile case which are 2x higher and lower as the default factor 100 applied in this study. All three acceleration factors resulted in a very similar bed development with very small differences of RMS=5 mm for factor 50 and 200 compared to factor 100. This is just 4% of the average scour depth at the end of the simulation. The RMS difference is determined for 360 locations (1 per degree) adjacent to the monopile for 19 flow files during the 5h scour development. These robust results justify the applied morphological acceleration factor of 100. To take morphological acceleration even a step further, also extreme factors 400 and 800 are tested. Acceleration factors 400 and 800 result in small differences of RMS=7 and 9 mm respectively compared to the factor 100 results, which is equivalent to 5% and 7% of the average scour at the end of the simulation.

Obviously, morphological speed-up shortens the computational time considerably. After spin-up of the turbulent flow, the round monopile CFD simulation took 5 days on 8 CPU cores (Intel Xeon CPU E3-1276 v3) for simulating 5 h scour development with morphological acceleration factor 100. For factor 200, 400, 800 this reduces to 2.5, 1.3, 0.7 days respectively. Using more CPU cores would also accelerate the computational time, since TUDflow3D runs efficiently in parallel. This brings application of process-based CFD scour simulations within reach for engineering projects, thus bringing CFD for scour development outside of the laboratory and into the real world.

CONCLUSION

Three experimental test cases are used to assess the quality of process-based LES CFD scour simulations with open-source software TUDflow3D, which employs morphological acceleration with a factor 100 to get results 100x faster. The three cases represent the scouring past a square and round monopile and a jacket foundation.

For all three cases accurate scour development was simulated for both the temporal and spatial development. The scour development at the side edges of the square and round monopile was reproduced more accurately than the scour upstream (angle=0°) or downstream (angle=180°) of the structure, although also at angle=0° and 180° the deviations between CFD and experiment are limited. A reason for this deviation might be, that the flow acceleration driven scouring is easier to simulate than the vortices driven scouring at the front and back. For the far more complex shape of a jacket foundation the simulated scour was also remarkably close to the experiment.

Sensitivity tests on grid resolution and morphological acceleration factor justify the initial choices in this study. In fact, they show that an even higher morphological factor of 200 could be used without compromising the quality of the results significantly. Using a morphological

acceleration factor of 100 for simulating five hours of scour development on lab-scale for the round monopile case, resulted in a computational duration of 5 days on an 8-core computer. Using factor 200 would bring this duration down to 2.5 days. It shows accurate process-based 3D CFD scour simulations are feasible for engineering projects when using morphological acceleration.

REFERENCES

- Baykal, C., Sumer, B. M., Fuhrman, D. R., Jacobsen, N. G., & Fredsøe, J. (2017). Numerical simulation of scour and backfilling processes around a circular pile in waves. *Coastal eng.*, 122, 87-107.
- Bagnold, R. A., (1966). An approach to the sediment transport problem from general physics. US government Print Office.
- Hinterberger, C. (2004) *Dreidimensionale und tiefengemittelte Large-Eddy-Simulation von Flachwasserströmungen*. Ph.D. Thesis, Universität Karlsruhe.
- Ikeda, S., (1982). “Incipient Motion of Sand Particles on Side Slopes.” *Journal of the Hydraulics Division*, ASCE 108 (1): 95–114.
- Jarrin, N., S. Benhamadouche, D. Laurence, and R. Prosser (2006). A synthetic-eddy-method for generating inflow conditions for LES. *Int. J. of Heat&Fluid Flow* 27(4), 585 – 593.
- Kim, H.S., Nabi, M., Kimura, I., Shimizu, Y. (2014), Numerical investigation of local scour at two adjacent cylinders, *Advances in Water Resources*, 70, 131–147
- Krajnovic, S. and L. Davidson (2002). Large-Eddy Simulation of the Flow Around a Bluff Body. *AIAA Journal* 40(5), 927–936.
- Krajnovic S. (2011). Flow around a tall finite cylinder explored by large eddy simulation. *Journal of Fluid Mechanics*, 676
- Manninen M., Taivassalo V. & Kallio S., (1996). *On the Mixture Model for Multiphase Flow*. VTT Publications 288. Technical Research Center of Finland.
- Nicoud, F. and F. Ducros (1999). Subgrid-Scale Stress Modelling Based on the Square of the Velocity Gradient Tensor. *Flow, Turbulence and Combustion* 62(3), 183–200.
- Radermacher M., De Wit L., Winterwerp J.C. & Uijttewaalt W.S.J., (2016). Efficiency of hanging silt screens in crossflow. *J. of Waterway, Port, Coastal and Ocean Engineering*, 142 (1).
- Rijn, L.C. van, (1984). Sediment pick-up functions, *Journal of Hydraulic Engineering*, 110(10).
- Rijn, L.C. van, (2007). Unified View of Sediment Transport by Currents and Waves. I: Initiation of Motion, Bed Roughness, and Bed-Load Transport, *Journal of Hydraulic Engineering*, 133(6).
- Rodi, W. (1998). Large-Eddy Simulations of the flow past Bluff Bodies: State-of-the-Art. *JSME Int. Journal* 41(2), 361–374.
- Roulund, A., Sumer, B.M., Fredsøe, J. and Michelsen, J., (2005). Numerical and experimental investigation of flow and scour around a circular pile. *J. FluidMech.* 534, 351–401
- Wit, L. de, van Rhee, C. (2014), Testing an improved artificial viscosity advection scheme to minimise wiggles in large eddy simulation of buoyant jet in crossflow, *Flow, Turbulence and Combustion*, 92(3):699 - 730.
- Wit, L. de (2015) *3D CFD modelling of overflow dredging plumes*. Ph.D. Thesis, Delft University of Technology, Delft.
- Yeon, S.M. (2014) *Large-eddy simulation of sub-, critical and super-critical Reynolds number flow past a circular cylinder*, Ph.D Thesis, University of Iowa